Chemistry Faculty Research and Scholarship   Chemistry

1987

Methyl Reorientation in Methylphenanthrenes: 1. Solid-State Proton Spin-Lattice Relaxation in the 3-Methyl, 9-Methyl, and 3,9-Dimethyl Systems

K. G. Conn

Peter A. Beckmann
Bryn Mawr College, pbeckman@brynmawr.edu

C. W. Mallory

Frank B. Mallory
Bryn Mawr College, fmallory@brynmawr.edu

Methyl reorientation in methylphenanthrenes. I. Solid state proton spin-lattice relaxation in the 3-methyl, 9-methyl, and 3,9-dimethyl systems[a),b)]

K. G. Conn and P. A. Beckmann
Department of Physics, Bryn Mawr College, Bryn Mawr, Pennsylvania 19010

C. W. Mallory
Department of Chemistry, University of Pennsylvania, Philadelphia, Pennsylvania 19104

F. B. Mallory
Department of Chemistry, Bryn Mawr College, Bryn Mawr, Pennsylvania 19010

We have investigated the dynamics of methyl group reorientation in solid methyl-substituted phenanthrenes. The temperature dependence of the proton spin–lattice relaxation rates has been measured in polycrystalline 3-methylphenanthrene (3-MP), 9-methylphenanthrene (9-MP), and 3,9-dimethylphenanthrene (3,9-DMP) at Larmor frequencies of 8.50, 22.5, and 53.0 MHz. The data are interpreted using a Davidson–Cole spectral density which implies either that the correlation functions for intramolecular reorientation are nonexponential or that there is a distribution of exponential correlation times. Comparing the fitted parameters that characterize the relaxation data for the three molecules shows that the individual contributions to the relaxation rate from the 3- and 9-methyls in 3,9-DMP can be separated and that the parameters specifying each are similar to the equivalent group in the two single methylphenanthrenes. The 9-methyl group is characterized by effective activation energies of 10.6 ± 0.6 and 12.5 ± 0.9 kJ/mol in 9-MP and 3,9-DMP, respectively, whereas the 3-methyl group is characterized by effective activation energies of 5.2 ± 0.8 and 5 ± 1 kJ/mol in 3-MP and 3,9-DMP, respectively. The agreement between the fitted and calculated values of the spin–lattice interaction strength, assuming only intramethyl proton dipole–dipole interactions need be considered, is excellent. A comparison between experimentally determined correlation times and those calculated from a variety of very simple dynamical models is given, and the results suggest, as have several previous studies, that at high temperatures where tunneling plays no role, methyl reorientation is a simple, thermally activated, hopping process. We have also analyzed many published data in methyl-substituted phenanthrenes, anthracenes, and naphthalenes (14 molecules) in the same way as we did for the phenanthrene data presented here, and a consistent picture for the dynamics of methyl reorientation emerges.

INTRODUCTION

Nuclear spin relaxation experiments have proved to be an excellent way to probe the dynamics of intramolecular reorientation of substituent groups in molecular solids. The combination of experimental results and dynamical models can provide insight into both the local anisotropic electrostatic potentials and the fundamental nature of the reorientation process.[1] In this paper we report solid-state proton spin–lattice relaxation measurements as a function of temperature at three Larmor frequencies in 3-methylphenanthrene (3-MP), 9-methylphenanthrene (9-MP), and 3,9-dimethylphenanthrene (3,9-DMP) as shown in Figs. 1, 2, and 3. The observed relaxation rate is $R \sim AJ(\omega, x_1, x_2,...)$, where the parameter A characterizes the time-independent strength of the spin–lattice interaction and J is a spectral density that characterizes the modulation of the spin–lattice interaction by the motion of the methyl substituents. J, in turn, is characterized by the nuclear Larmor angular frequency ω and a parameter set $\{x_i\}$ that characterizes the intramolecular motion. The nuclear spins relax via the Larmor frequency Fourier component of the local oscillating magnetic field, and since the Larmor angular frequency $\omega = \gamma B$ (for magnetogyric ratio γ and magnetic induction B) is determined by the laboratory magnet, the experimenter has direct control over which Fourier component of the motion is being observed. In the present case, it is the methyl group reorientation that provides the relevant time dependence of the local magnetic field. For the parameter set that characterizes the motion, a single $x_1 = \tau$ is assumed in the simplest case where the correlation time τ characterizes the intramolecular dynamics. The correlation time τ is a statistical parameter and contains information about the electrostatic potential experienced by the methyl group. In general, there will be other parameters $x_2, x_3,...$, that are strongly model dependent, and that characterize other aspects of the molecular motion in the solid state. At least some of these parameters will depend on temperature, and the fundamental problem in dynamic solid-state NMR is to determine and interpret the form of the spectral density $J\{\omega, x_1(T,...), x_2(T,...),...\}$. Spin–lattice relaxation measurements give too few experimentally determined parameters to severely test
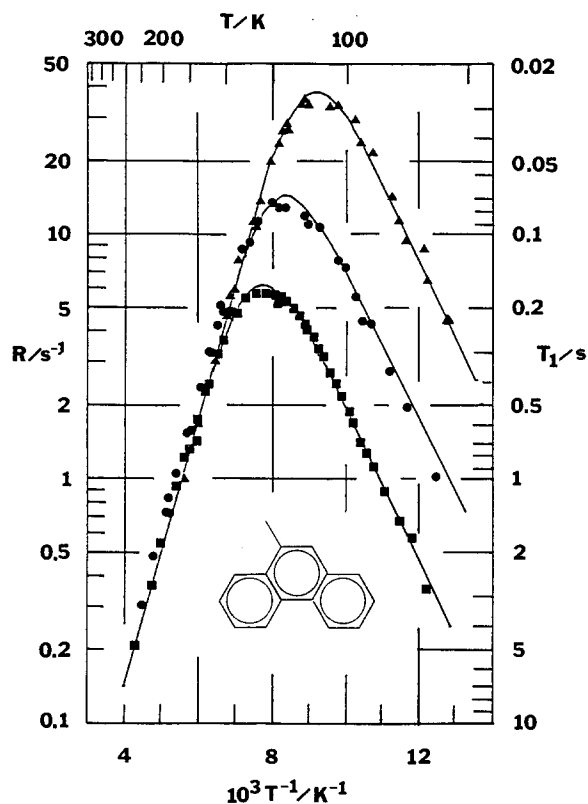
FIG. 1. ln(R) vs T^{-1} in 9-methylphenanthrene (9-MP) at 8.50 (▲), 22.5 (●), and 53.0 MHz (■). The solid lines are the theoretical fits. A schematic picture of the molecule is shown in the inset.

FIG. 2. ln(R) vs T^{-1} in 3-methylphenanthrene (3-MP) at 8.50 (▲) and 53.0 MHz (■). The solid lines are the theoretical fits. A schematic picture of the molecule is shown in the inset.

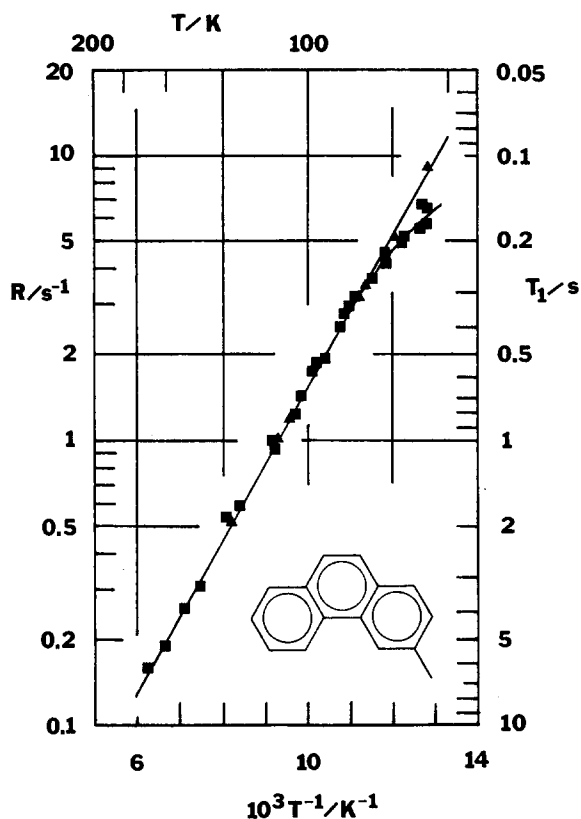realistic models for the reorientational dynamics of subunits like methyl groups. In order to build complete self-consistent models, nuclear spin relaxation experiments must be coupled with other structural and dynamical techniques such as neutron scattering,[2,3] x-ray diffraction,[4] and microwave spectroscopy.[5]

Organic molecular solids containing two or more aromatic rings provide ideal molecular laboratories for the pursuit of these studies. Examples of useful molecules are the methyl-substituted naphthalenes,[6,7] anthracenes,[8] phenanthrenes,[4] and chrysenes.[9] There are many reasons for studying these systems. First, the molecular backbones are sufficiently large and rigid that whole-molecule translation and reorientation does not occur on the nuclear Larmor frequency time scale. For most of these systems, this is true even at temperatures very close to the melting point. This means that methyl reorientation is the only motion that contributes significantly to nuclear spin relaxation and this simplifies comparisons between theory and experiment. Second, most of these systems have single, well-defined solid phases throughout the temperature range of interest. This is not true of many methyl-substituted benzenes (single ring compounds), which can have large thermal history effects[10] and which can undergo solid–solid phase transitions with, in some cases, large hysteresis effects typical of glassy states.[11–15] Third, methyl reorientation is a one-dimensional process and it is not difficult to solve Schrödinger's equation for a wide variety of rotational barriers.[16] Fourth, the strength constant A can be calculated exactly if it is assumed
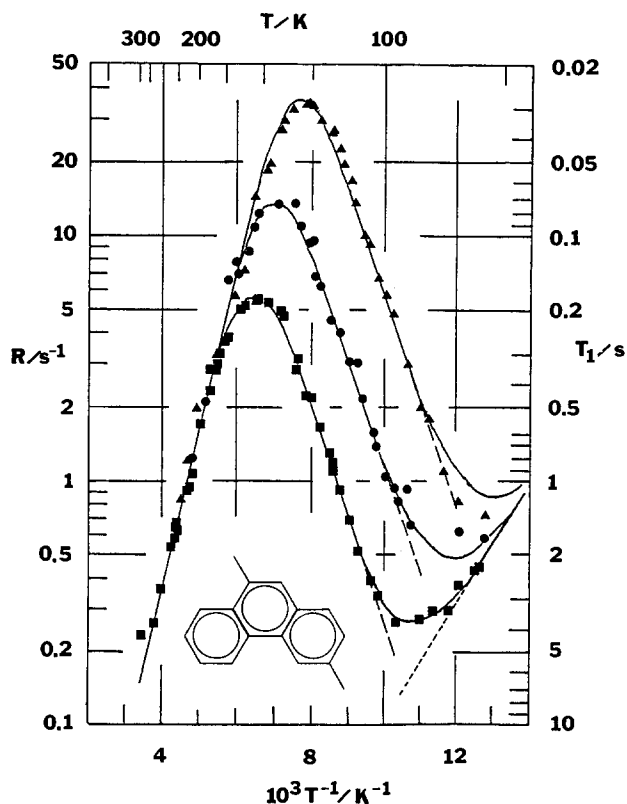
FIG. 3. ln(R) vs T^{-1} in 3,9-dimethylphenanthrene (3,9-DMP) at 8.50 (▲), 22.5 (●), and 53.0 MHz (■). The dashed and dotted lines give the theoretical fits for the 9- and 3-methyl groups, respectively. The solid lines are the sums of the two contributions. A schematic picture of the molecule is shown in the inset.

TABLE I. Relaxation rate parameters.

Molecule[a]	Methyl groups	Type	#ω's	E (kJ/mol)	$A/\tilde{A}$	ϵ	$\tau_\infty/\tilde{\tau}_\infty$	Ref.
9-MP	9	α	3	10.6	0.98	0.57	1.01	...
3,9-DMP	9	α	3	12.5	0.98	0.68	1.12	...
	3	β	3	5	...	...	$(0.1)^b$	...
3-MP	3	β	2	5.2	...	...	$(1.4)^b$	...
4-MP	4	...	1	21	1.0	1.0	1.12	4
4,5-DMP[c]	4,5	...	1	10	0.88	0.91	0.82	4
1-MA	1	α	1	9.6	1.0	1.0	0.64	8
1,10-DMA	1	α	1	15.7	...	...	$(0.67)^b$	8
	10	...	1	<3	...	...	...	8
1-MN[d]	1	α	4	9.1	1.43	0.24	2.97	6
2-MN	2	β	4	4	...	...	$(0.22)^b$	6
1,3-DMN	1	α	4	8.8	1.16	0.34	1.67	6
1,5-DMN	1,5	α	4	9.5	1.0	0.88	1.1	6
	1,5	α	1	9.6	1.0	1.0	0.99	7
1,7-DMN	1	α	4	10.6	0.91	0.59	0.93	6
1,8-DMN	1,8	...	4	13.4	...	...	...	6
	1,8	...	1	13.5	1.0	1.0	0.99	7
2,3-DMN	2,3	...	4	9.4	1.19	0.35	0.96	6
2,6-DMN	2,6	β	4	1.7	...	...	$(0.86)^b$	6
2,3,6-TMN	2,3	...	4	8.6	~1	~0.3	~2	6
1,4,5,8-TMN	1,4,5,8	...	1	14.6	1.15	1.0	1.21	7

[a] Abbreviations: MP = methylphenanthrene, DMP = dimethylphenanthrene, MA = methylanthracene, DMA = dimethylanthracene, MN = methylnaphthalene, DMN = dimethylnaphthalene, TMN = trimethylnaphthalene or tetramethylnaphthalene.

[b] For these systems, only E can be determined since only the high temperature data characterized by Eq. (6) are observed. E comes from $\mathscr{A}$ [Eq. (11)] and a relationship between ϵ, A, and τ_∞ comes from Eq. (14). For comparison purposes, the quoted value of $\tau_\infty/\tilde{\tau}_\infty$ assumes that $A/\tilde{A} = 1$ and $\epsilon = 1$. This ratio is inversely proportional to ϵ.

[c] X-ray work (Ref. 4) suggests that the two methyls are inequivalent which means that the fit we have made here is not really justified.

[d] This is the only entry for which the fit to a Davidson–Cole distribution was very poor.

that the only nuclear dipole–dipole interactions of importance are intramethyl. The present experiments, along with others (see Table I), show that this is the case for the molecular systems discussed above. Fifth, in each of these ring systems, the large molecular backbone provides a convenient network of equivalent and inequivalent sites on which methyl groups can be placed. This allows comparisons (of the parameters that characterize methyl reorientation) between groups in the same molecular position in different molecules. Sixth, in the polycrystalline or powdered solids used in this and similar studies, there results a random distribution of methyl reorientation axes, which makes certain averaging procedures in the modeling of $J(\omega, \{x_i\})$ easier. It means one can use statistical ensemble theory to mimic random, isotropic reorientation as in a liquid.

The main results of the combination of this study and our review of previous work are twofold. First, the same spectral density is successful in a wide variety of organic molecular solids as indicated in Table I. This suggests that the fundamental description of the dynamics is correct or at least adequate. Second, either the correlation function for molecular reorientation is nonexponential or there is a distribution of correlation times, each characterizing a Poisson, or random, dynamical process.

THE EXPERIMENTS

Each methyl-substituted phenanthrene was prepared by oxidative photocyclization of the appropriate methyl-substi-

tuted stilbene.[17] The products were purified in each case by chromatography on alumina using hexane as the eluent, followed by recrystallization from methanol. The properties of the individual samples are as follows: 3-methylphenanthrene (3-MP), colorless needles, mp 60.8–62.0 °C (lit.[18] mp 62–63 °C); 9-methylphenanthrene (9-MP), colorless needles, mp 90.0–92.0 °C (lit.[19] mp 91.5–92.5 °C); 3,9-dimethylphenanthrene (3,9-DMP), colorless needles, mp 58.0–59.6 °C (lit.[20] mp 62 °C).

The samples were ground with a mortar and pestle and placed in 7 mm diam sample tubes for the proton spin–lattice relaxation measurements. Temperature was measured with a calibrated copper–Constantan thermocouple that was embedded inside the sample just outside the part of the sample that was located within the NMR coil. The Zeeman spin–lattice relaxation rates, R, were measured using a standard π-t-$(\pi/2)$-t_R pulse sequence with $t_R \geqslant 8R^{-1}$. For the methyl-substituted phenanthrenes, the free induction decays were very short ($T_2 \sim 10\,\mu$s), indicating rapid spin diffusion. The relaxation was always exponential within the experimental uncertainties. The rates R were measured as a function of temperature T at magnetic field intensities of 0.200, 0.530, and 1.25 T corresponding to proton Larmor frequencies of 8.50, 22.5, and 53.0 MHz.

Plots of $\ln(R)$ as a function of T^{-1} are shown in Figs. 1, 2, and 3. There is one rotor site in 9-MP (Fig. 1), one in 3-MP (Fig. 2), and two inequivalent sites in 3,9-DMP (Fig. 3). For 3,9-DMP, the observed maximum in R is due to the

9-methyl group, and the low temperature departure from a linear $\ln(R)$ vs T^{-1} dependence is due to the 3-methyl group.

REVIEW OF THE THEORY

The observed Zeeman spin–lattice relaxation rates R in Figs. 1, 2, and 3 result from the modulation of proton dipole–dipole interactions due to the reorientation of methyl groups about their threefold axes. R is given by[1]

$$R = A[J_1(\omega, x_1, x_2, \dots) + 4J_2(2\omega, x_1, x_2, \dots)],\qquad (1)$$

where the parameter A characterizes the strength of the various dipole–dipole interactions. If these interactions are dominated by the three pair-wise intramethyl interactions, and if it is assumed that rapid spin diffusion relaxes all protons in the molecule,[21] then the parameter A can be calculated. We specify this calculated value of A by $\tilde{A}$ and it is given by[22]

$$\tilde{A} = \frac{9}{40}\frac{n}{N}\left[\frac{\mu_0}{4\pi}\right]^2 \frac{\gamma^4\hbar^2}{r^6}.\qquad (2)$$

The proton–proton separation in a methyl group is r, $\mu_0/(4\pi) = 10^{-7}\ \mathrm{m\ kg^{-2}\,A}$ where μ_0 is the permeability of free space, the proton magnetogyric ratio is $\gamma = 2.675 \times 10^8\ \mathrm{kg^{-1}\,s\,A}$, and $\hbar = 1.054 \times 10^{-34}\ \mathrm{m^2\ kg\ s^{-1}}$. By assuming $r = 1.797 \times 10^{-10}$ m, the parameter $\tilde{A} = (n/N)3.80 \times 10^9\ \mathrm{s^{-2}}$. $\tilde{A}$ can be interpreted as the strength of the spin–lattice coupling due to the intramethyl proton dipole–dipole interactions, diluted by n/N, which is the the ratio of the number of protons in methyl groups involved in the motion to the number of protons in the molecule. For 3-MP and 9-MP, $n = 3$ and $N = 12$. For both the 3- and the 9-methyl groups in 3, 9-DMP (which can be considered separately), $n = 3$ and $N = 14$. If dipole–dipole interactions between methyl protons and other protons are important, A in Eq. (1) will be larger than $\tilde{A}$ in Eq. (2) but $\tilde{A}$ gives a lower limit for A. The effects of neighboring protons cannot be judged solely by the magnitudes of the proton-proton vectors involved since it is the modulation of both the magnitude and orientation of these vectors that matters. For example, when a methyl group reorients via a single jump, each intramethyl proton–proton vector reorients by 120°, but other proton–proton vectors change their orientation by less so the effect of the latter ones on the spin–lattice relaxation is reduced.

The form of the normalized spectral densities J_k in Eq. (1) and the relationship between the molecular parameters x_i and the temperature T (or some other experimental variable such as the pressure) is one of the more important and fascinating problems for nuclear spin relaxation studies. We assume that $J_1 = J_2$. This assumption is certainly not justified in systems like liquid crystals where some relaxation mechanisms, like order director fluctuations, contribute to J_1 and not J_2.[23] However, these conditions do not prevail in the finely ground powdered samples used in this and other related studies.

It is convenient to define a correlation time via an Arrhenius relationship,

$$\tau(T, E, \tau_\infty) = \tau_\infty e^{E/kT},\qquad (3)$$

in which case,

$$J = J(\omega, T, E, \tau_\infty, x_4, x_5, \dots)$$
$$= J[\omega, \tau(T, E, \tau_\infty), x_4, x_5, \dots].\qquad (4)$$

In a sense, Eq. (3) is artificial because τ_∞ will, in general, depend slightly on temperature. An estimate for τ_∞ (which we call $\tilde{\tau}_\infty$) can be obtained by assuming that the potential is a simple sinusoid of peak-to-peak height $E \gg kT$ and that thermally activated rotation over the top of the barrier is strongly hindered. The reorientation rate τ^{-1}, the inverse of τ in Eq. (3), is the product of the probability of being near the top of the well, $\exp(-E/kT)$, and the attempt frequency, τ_∞^{-1} (i.e., the frequency the rotor has when it does happen to be near the top of the well). In the harmonic approximation, this attempt frequency may be approximated by the vibrational frequency $\tilde{\tau}_\infty^{-1}$ given by[5]

$$\tilde{\tau}_\infty = \left(\frac{2\pi}{3}\right)\left(\frac{2I}{E}\right)^{1/2},\qquad (5)$$

where I is the moment of inertia for a methyl group and has the value $5.3 \times 10^{-47}\ \mathrm{kg\ m^2}$. This model seems totally unrealistic but is surprisingly accurate. The reason for this is not because the assumed model is correct, which is clearly not the case, but because more realistic models predict values of τ_∞ not so very different from $\tilde{\tau}_\infty$ in Eq. (5). We shall investigate two such models after discussing the relaxation rate data in detail. In any event, Eq. (3) can be taken as the defining equation for the parameters E and τ_∞, and $\tilde{\tau}_\infty$ in Eq. (5) is a convenient benchmark with which to compare τ_∞.

DATA ANALYSIS AND DISCUSSION

As seen in Figs. 1 and 3, our data for 9-MP and 3,9-DMP exhibit maxima in the plots of $\ln(R)$ vs T^{-1} at each frequency. Each plot shows regions of linearity at temperatures both above and below those in the immediate vicinity of the maximum. The high temperature linear region is characterized by a positive slope $\mathscr{A}$ and a positive intercept $\mathscr{B}$.

$$\ln(R) = \mathscr{A}T^{-1} + \mathscr{B}.\qquad (6)$$

The low temperature linear region is characterized by a negative slope $-\mathscr{C}$ (with $\mathscr{C} > 0$) and a positive intercept $\mathscr{D}$.

$$\ln(R) = -\mathscr{C}T^{-1} + \mathscr{D}.\qquad (7)$$

For 3,9-DMP it is assumed that the observed maximum in R is due to the reorientation of the 9-methyl group. The upward deviation from linearity at the lowest temperatures is assumed to be due to the reorientation of the 3-methyl group. In using the data to obtain $\mathscr{C}$ and $\mathscr{D}$ for the 9-methyl group, then, only the linear portion of the low temperature data is used. The four positive constants $\mathscr{A}$, $\mathscr{B}$, $\mathscr{C}$, and $\mathscr{D}$ are convenient fitting parameters although we shall replace this set by another set below. We note that this parameterization does not specify $\ln(R)$ vs T^{-1} in the vicinity of the maximum in R.

Before returning to the general analysis of the data, we note that a key feature of our results is that the $\ln(R)$ vs T^{-1} data in Figs. 1 and 3 cannot be fit by a Lorentzian spectral density,[1]

$$J(\omega,\tau) = \frac{2\tau}{1 + \omega^2\tau^2}, \tag{8}$$

which follows from the assumption of random motion characterized by a single correlation time τ.[1,24,25] Equation (8), used in conjunction with Eqs. (1) and (3), requires that $\mathscr{A} = \mathscr{C}$ as will be evident later. For the data in Figs. 1 and 3, $\mathscr{C}$ is significantly less than $\mathscr{A}$.

By inspection of Figs. 1 and 3, it can be seen that of the four parameters $\mathscr{A}$, $\mathscr{B}$, $\mathscr{C}$, and $\mathscr{D}$, the only one that depends on the Larmor angular frequency ω is $\mathscr{D}$. Further, the analysis of our data and most of the published data summarized in Table I shows that there is a specific relationship between $\mathscr{C}/\mathscr{A}$, the ratio of the magnitudes of the slopes, and the dependence of $\mathscr{D}$ on ω. If the constant parameter ϵ is defined by

$$\epsilon = \mathscr{C}/\mathscr{A}, \tag{9}$$

then the relationship between $\mathscr{D}$ and ϵ is

$$e^{\mathscr{D}} = \mathscr{F}\omega^{-1-\epsilon}, \tag{10}$$

where $\mathscr{F}$ is a positive constant independent of ω. To express the frequency dependence in another way, at low temperatures, where the data are characterized by Eq. (7), $R \propto \omega^{-1-\epsilon}$ where ϵ can be determined from $\ln(R)$ vs T^{-1} at any one ω via Eq. (9). Finally, we define the constant parameter E by

$$\mathscr{A} = E/k, \tag{11}$$

where k is Boltzmann's constant. It follows that

$$\mathscr{C} = \epsilon E/k, \tag{12}$$

and all the data in the high and low temperature linear regions at all three frequencies in Figs. 1 and 3 (excluding the deviations from linearity at the lowest temperatures for the latter) can be completely characterized by the four constants $E, \epsilon, \mathscr{B}$, and $\mathscr{F}$. We emphasize that this parameterization is independent of the form of the spectral density. This is the simplest data reduction procedure possible and it does not include parameterization of the data in the vicinity of the maximum in R.

In molecular solids, it is quite common to observe values of $R(T,\omega)$ that can be characterized by the the four constants $E, \epsilon, \mathscr{B}$, and $\mathscr{F}$ discussed above; many examples are included in Table I. We have previously given a general discussion[26] of the mathematical properties that the spectral density J must have in order to fit data like these. There are many classes of such functions, and finding a unique and universal $J(\omega,T,x_2,x_3,...)$ (or determining if one exists) is an important problem for the future. At this time we must be content with phenomenological spectral densities, with the hope that by comparing the experimental results in a variety of related molecular systems, we can learn better how to incorporate realistic electrostatic potentials for the solid state in the theoretical calculation of the spectral density. We have chosen to fit our data in Fig. 1 to the spectral density due to Davidson and Cole,[27]

$$J(\omega,\tau) = \frac{2}{\omega}\frac{\sin[\epsilon\arctan(\omega\tau)]}{(1+\omega^2\tau^2)^{\epsilon/2}}, \tag{13}$$

where $0 < \epsilon \leqslant 1$. When $\epsilon = 1$, the Davidson–Cole spectral density in Eq. (13) reduces to the Lorentzian spectral den-

sity in Eq. (8). We have also chosen to use the Arrhenius relationship of Eq. (3) to represent the correlation time τ. The expression for R is given by Eqs. (1), (13), and (3) and the four theoretical parameters are A in Eq. (1), E and τ_∞ in Eq. (3), and ϵ in Eq. (13). The parameters E and ϵ already appear in the spectral density-independent fitting procedure discussed previously. It remains to relate the experimental parameter pair ($\mathscr{B}, \mathscr{F}$) to the theoretical parameters. It is straightforward to show that

$$\mathscr{B} = \ln(10A\epsilon\tau_\infty) \tag{14}$$

and

$$\mathscr{F} = 2A\left\{1 + 2^{1-\epsilon}\right\}\{\sin(\epsilon\pi/2)\}\tau_\infty^{-\epsilon}. \tag{15}$$

Given that the values of $\mathscr{A}$, $\mathscr{B}$, $\mathscr{C}$, and $\mathscr{D}$ in Eqs. (6) and (7) are obtained from the data in Figs. 1 and 3, the fitting procedure is to first determine E from Eq. (11), then ϵ from Eq. (12), then A and τ_∞ from Eqs. (10), (14), and (15). The determinations of E for the 9-methyl groups in 3,9-DMP and 9-MP are found to give very similar values of 12.5 ± 0.9 kJ/mol and 10.6 ± 0.6 kJ/mol, respectively. The parameter ϵ is found to be less than one and this will be discussed in the next section. The fitted values of A and τ_∞ for the 9-methyl groups in 9-MP and 3,9-DMP are given in Table I via the ratios $A/\tilde{A}$ and $\tau_\infty/\tilde{\tau}_\infty$. $\tilde{A}$ is given by Eq. (2) and $\tilde{\tau}_\infty$ is given by Eq. (5). The fact that the ratios $A/\tilde{A}$ are near unity suggests that only intramethyl proton dipole–dipole interactions are important for spin–lattice relaxation in these systems. The ratios $\tau_\infty/\tilde{\tau}_\infty$ are also close to unity and this will be discussed in the next section. Finally, we note that this analysis fits the relaxation rates (resulting from the reorientation of the 9-methyl groups) in the vicinity of the maximum in R very well as shown in Figs. 1 and 3. In summary, the Davidson–Cole spectral density with the correlation time given by an Arrhenius relationship fits the data very successfully.

For the 3-methyl group in both 3-MP and 3,9-DMP we are unable to measure the low temperature region of the spin–lattice relaxation rate (see Figs. 2 and 3) because our experimental capabilities at present do not extend below 77 K; therefore the only quantity we can evaluate explicitly in these systems is E, which is determined from the high temperature frequency-independent slope. For 3-MP, obtaining E from Eq. (11) is straightforward. The contribution of the 3-methyl group to the overall relaxation rate in 3,9-DMP was evaluated by extrapolating to lower temperatures the linear parts of the frequency-dependent low temperature data for the 9-methyl group as plotted in Fig. 3, and by calculating the differences between the experimental values of $\ln(R)$ and the values of $\ln(R)$ along these three extrapolated lines. Because of the limited low temperature data at 22.5 and 8.5 MHz, this procedure is only really meaningful for the data at 53 MHz. However, the differences in $\ln(R)$ vs T^{-1} calculated from the data at 53 MHz are consistent with these same differences calculated from the data at the other frequencies. It is also consistent with a low temperature frequency-independent contribution to $\ln(R)$ vs T^{-1} as expected. The value of E for the 3-methyl group in 3,9-DMP which results from this analysis is 5 ± 1 kJ/mol. As indicated in Table I, this value is the same as the value of $E = 5.2 \pm 0.7$

kJ/mol determined for the 3-methyl group in 3-MP. These values are significantly lower than the values of E for the 9-methyl groups in 3,9-DMP and 9-MP.

In order to compare our results with those in other systems, we have fitted published R vs T data in methyl-substituted phenanthrenes,[4] anthracenes,[8] and naphthalenes[6,7] to the Davidson–Cole spectral density. The results are shown in Table I. In general the fits are very good although some published data are not fitted well in the vicinity of the maximum in R. The number of frequencies employed in each experiment is listed in Table I. No values are tabulated for A, ϵ, and τ_∞ if only the high temperature data were observed (as, for example, for the 3-methyl group in both 3-MP and 3,9-DMP). In Table I, we use the label α to designate the type of methyl group that is flanked intramolecularly by a peri hydrogen on one side and an ortho hydrogen on the other side (as in 9-MP), and we use the label β to designate the type of methyl group that is flanked intramolecularly by ortho hydrogens on both sides (as in 3-MP). Most α methyls are sufficiently strongly hindered by crowding against the adjacent peri hydrogen that the apparent activation energy E lies between about 9 and 13 kJ/mol, and the regions corresponding to both $\omega\tau \ll 1$ and $\omega\tau \gg 1$ can usually be observed in spin–lattice relaxation experiments. For such systems, the parameters A, ϵ, and τ_∞ can be determined, and (except for the anomalous case of 1-methylnaphthalene) the Davidson–Cole spectral density works well with $A/\tilde{A}$ values near unity. This clearly indicates that intramethyl spin–spin interactions dominate the relaxation. For β-methyl groups, E ranges from about 2 to 5 kJ/mol, indicating less hindered rotation as expected. For most of the data involving β-methyl groups, it is not possible to determine the spectral density because only the high temperature region corresponding to $\omega\tau \ll 1$ has been observed.

Because the methyl groups in these molecules behave in such an ideal fashion from the point of view of interpreting the nuclear spin–lattice relaxation experiments, we shall pursue further the interpretation of the Arrhenius relationship in Eq. (3). A straightforward quantum mechanical approach that assumes a thermally activated hopping process to describe the methyl reorientation at high temperatures seems to have all the qualitative and quantitative features required to interpret the data.[28] The quantum mechanical problem is that of a single one-dimensional rotor.[16] With a threefold sine function potential, the Schrödinger equation can be solved numerically for a given barrier height. If the E values measured here for the phenanthrenes are taken as the barrier heights and a sinusoidal potential is assumed, then there will be at least several bound rotational states for the 3-methyl groups in 3-MP or 3,9-DMP and many bound rotational states for the more strongly hindered 9-methyl groups in 9-MP and 3,9-DMP. For completeness, we note that if there are significantly different well depths that are appreciably populated, the usual effect is to make the high temperature slope in a plot of $\ln(R)$ vs T^{-1} smaller than the low temperature slope[29]; this behavior is rarely observed in systems where only single motions are occurring, and it is never observed, to our knowledge, for large immobile organic molecules with relatively small reorienting groups.

The simplest dynamical model assumes that τ is given by Eq. (3) with τ_∞ given by $\tilde{\tau}_\infty$ in Eq. (5). This model has been discussed above and is compared with the data in Table I by giving the fitted values of τ_∞ in terms of $\tau_\infty/\tilde{\tau}_\infty$. As shown in Table I, the data are remarkably well fitted by this oversimplified model. This success is not so surprising when one looks at more realistic models.[30–35] These various models show that the general problem is very complicated. Some of them show why the relaxation rates are not very sensitive to the detailed shape of the barrier so long as it has (at least) threefold symmetry and the barrier height $V \gg kT$. In addition, Kowalewski and Liljefors[32] have shown that for barrier heights of 8 and 14 kJ/mol, the activation energy computed from absolute rate theory is very close to the potential barrier height. The authors caution, however, that this result is not obvious and occurs because of cancellations of certain terms in the theory.

In order to show how the Arrhenius relationship in Eq. (3), with τ_∞ of the order of $\tilde{\tau}_\infty$ given by Eq. (5), occurs naturally in models that are somewhat more realistic than the model that assumes a strongly hindered rotor with a harmonic oscillator attempt jump rate, we consider the case of a continuum of rotational levels with a uniform density of states, including levels above the barrier. Using this approach, Clough and Heidemann[31] performed a calculation of limiting values for the reorientation rate τ^{-1}. They assumed a sawtooth barrier of height E for one example and a square barrier of height E and wells and barriers of equal width for another example. They calculated the correlation time τ for these models and they argued that a more realistic sine wave barrier would lie somewhere in between the two. They associated the correlation frequency τ^{-1} with the canonical ensemble average (assuming a uniform density of states) of the rate of $2\pi/3$ hops. The arguments and the resulting approximate but quite accurate closed form expressions for τ are elegant in their simplicity. For both a sawtooth barrier and a square barrier, Clough and Heidemann find that[31]

$$\tau = \tau_\infty^* \exp\left(\frac{E}{kT}\right), \tag{16}$$

where for a sawtooth barrier,

$$(\tau_\infty^*)^{-1} = \frac{3}{2\pi}\left[\frac{E}{2I}\right]^{1/2}\left\{1 + \frac{x}{2} - \frac{x^2}{4} + \left(\frac{\pi x}{4}\right)^{1/2}\right\} \tag{17}$$

and for a square barrier,

$$(\tau_\infty^*)^{-1} = 3\left\{\frac{kT}{2\pi I}\right\}^{1/2}$$

$$\times \left\{1 + \frac{3x}{2} + \frac{15x^2}{4} - \left(\frac{x}{\pi}\right)^{1/2}(1 + x)\right\}, \tag{18}$$

with $x = kT/E$. In the limit $E \gg kT$, τ_∞^* in Eq. (17) is identical to $\tilde{\tau}_\infty$ in Eq. (5) and, as seen below, τ_∞^* in Eq. (18) differs from $\tilde{\tau}_\infty$ by at most a factor of 6 and usually (i.e., at most temperatures) much less. The experimentally fitted parameter τ_∞ can now be compared with the values of τ_∞^* predicted by these models. Given the range of temperature used in the experiments reported here, the parameter x ranges from 0.05 to 0.21 for the 9-methyl group and from

0.12 to 0.25 for the 3-methyl group. With $\tilde{\tau}_\infty$ defined by Eq. (5), the resulting parameters τ_∞^* vary from 0.65 $\tilde{\tau}_\infty$ to 0.73 $\tilde{\tau}_\infty$ for the 3-methyl group using the sawtooth barrier, from 0.90 $\tilde{\tau}_\infty$ to 2.32 $\tilde{\tau}_\infty$ for the 3-methyl group using the square barrier, from 0.67 $\tilde{\tau}_\infty$ to 0.81 $\tilde{\tau}_\infty$ for the 9-methyl group using the sawtooth barrier and from 1.2 $\tilde{\tau}_\infty$ to 5.9 $\tilde{\tau}_\infty$ for the 9-methyl group using the square barrier. In order to investigate the ratios $\tau_\infty / \tau_\infty^*$, rather than the ratios $\tau_\infty / \tilde{\tau}_\infty$ (Table I), a more sophisticated fitting procedure would have to be used since the τ_∞^* are temperature dependent. However, because the values of τ_∞^* in Eqs. (17) and (18) are relatively insensitive to temperature [compared with the exponential factor in Eq. (16)] there would be no significant difference between this procedure and one which simply uses a value of τ_∞^* obtained from averaging over the relevant temperature range. In practice one need only divide the present numbers in the column labeled $\tau_\infty / \tilde{\tau}_\infty$ by a suitable average of the factors multiplying the $\tilde{\tau}_\infty$ given above. We conclude that all the models considered work quite well, and also that these kinds of experiments are relatively insensitive to the details of the model. More detailed discussions and more complex models concerning Eq. (3) and the meaning of τ_∞ can be found,[30,32–34] but employing these models seems unwarranted at this time. The point to be emphasized is that when only one model is employed, the agreement between experiment and theory is not a strong test of the theory.

SUMMARY AND FURTHER COMMENTS

Methyl-substituted phenanthrenes and other multiple-ring organic molecules provide excellent systems for the study of fundamental aspects of methyl reorientation as well as phenomenological approaches to the classification of rotor types in the solid state. Since the dynamical properties being probed by the nuclear spin–lattice relaxation experiments are very sensitive to the anisotropies in the local electrostatic potential, these studies, in conjunction with other techniques, aid in the determination of the anisotropic electrostatic interactions in molecular solids.

In this paper we have investigated the reorientation of the 3-methyl and 9-methyl groups in 3-MP, 9-MP, and 3,9-DMP. From the phenomenological point of view, the parameters used to characterize the dynamics show that both types of rotors (3-methyl and 9-methyl) are hindered and that the difference between the activation energies for the two types is large compared with the difference between the activation energies for the same types in different molecules. In looking at data for a series of systems, we find that α-methyl groups have activation energies in the range of 9 to 13 kJ/mol, whereas β-methyl groups have activation energies in the range of 2 to 5 kJ/mol as outlined in Table I.

In addition to the problem of understanding the magnitudes and the origins of the electrostatic molecular potentials, there is the general problem of providing adequate models for the reorientational dynamics of methyl groups. Solids are the best samples to use for this because the temperature range is very large and the motion of interest can be isolated. We have looked at several oversimplified but easy-to-handle models for the reorientation of methyl groups; considering their simplicity, these models all agree surpris-

ingly well with the experimental data. It seems clear that methyl reorientation is a thermally activated process for these rotors, and that the random hopping picture[28,36,37] contains all the salient features needed to describe the dynamics. The appealing aspect of this approach is that from the purely theoretical point of view, there are only two parameters, an activation energy (or a barrier height) and the temperature of the heat bath with which the methyl groups are in thermal contact.[28] There seems to be no need to introduce details concerning the structure of the reservoir (e.g., the phonon spectrum), only its temperature matters. Also, at temperatures above about 50 K, there is no need to take quantum mechanical tunneling into account.[37,38] Finally, there seems no need to include other nuclear spin–molecular rotation quantum effects[39–41] to interpret our results or those of many other related systems.

There remains the interpretation of the parameter ε, which, from the model-independent point of view, can be taken to be the ratio of the absolute magnitudes of the low to high temperature slopes in the observed $\ln R$ vs T^{-1} data. In many theoretical models, such as the Davidson–Cole model[27] used here, this parameter is related to a distribution of correlation times but this interpretation assumes that there are subensembles of rotors and the rotors within each subensemble are characterized by a Lorentzian spectral density. In this scenario, the spectral density used to fit the data arises because there is a distribution of subensembles or, equivalently, a distribution of Lorentzians via

$$J(\omega, x_1, x_2,...) = \int_0^\infty \Lambda(\tau', x_1, x_2,...)\frac{2\tau'}{1 + \omega^2(\tau')^2} d\tau'. \quad (19)$$

In the case of the Davidson–Cole distribution, Eq. (13) follows from Eq. (19) with[27]

$$\Lambda[\tau', \tau(\tau_\infty, E), \varepsilon] = \sin(\varepsilon\pi)\frac{1}{\pi\tau'}\left(\frac{\tau'}{\tau - \tau'}\right)^\varepsilon, \quad \tau' < \tau;$$
$$= 0 \qquad\qquad\qquad \tau' > \tau$$
$$\qquad\qquad\qquad\qquad\qquad\qquad\qquad (20)$$

In Eq. (20), $\tau(\tau_\infty, E)$ is a cutoff correlation time. This distribution may make physical sense if the intermolecular electrostatic potential plays a significant role. That is, there very well may be a distribution of environments with the cutoff $\tau' = \tau$ associated with methyl groups that have "normal" or "the most likely" crystalline environment; other methyl groups might be located in freer environments for reorientation owing to crystal imperfections and crystallite boundaries. A room temperature powder x-ray study of 3,9-DMP showed that the sample was polycrystalline and not amorphous or glassy.

Another interpretation of this distribution of correlation times is that it may just be convenient bookkeeping. If the correlation function for molecular reorientation is inherently nonexponential then the spectral density in Eq. (19) is just a convenient way of representing a non-Lorentzian spectral density.[14] In this case, the correlation function, instead of being $\exp(-|t|/\tau)$, which is the Fourier transform of the Lorentzian spectral density in Eq. (8), is

$$G(t, x_1, x_2,...) = \int_0^\infty \Lambda(\tau', x_1, x_2,...)e^{-|t|/\tau'} d\tau'. \quad (21)$$

It remains a problem of fundamental importance and of great interest to distinguish between these two interpretations.

ACKNOWLEDGMENTS

[1] C. P. Slichter, *The Principles of Magnetic Resonance* (Springer, Berlin, 1978).

[2] A. Heidemann, S. Clough, P. J. McDonald, A. J. Horsewill, and K. Neumaier, Z. Phys. B **58**, 141 (1985).

[3] B. Gabryś, J. S. Higgins, K. T. Ma, and J. E. Roots, Macromolecules **17**, 560 (1984).

[4] K. Takegoshi, F. Imashiro, T. Terao, and A. Saika, J. Chem. Phys. **80**, 1089 (1984).

[5] N. L. Owen, in *Internal Rotation in Molecules*, edited by W. J. Orville-Thomas (Wiley, New York, 1974), p. 157.

[6] J. U. von Schültz and H. C. Wolf, Z. Naturforsch. Teil A **27**, 42 (1972).

[7] F. Imashiro, K. Takegoshi, S. Okazawa, J. Furukawa, T. Terao, and A. Saika, J. Chem. Phys. **78**, 1104 (1983).

[8] K. Takegoshi, F. Imashiro, T. Terao, and A. Saika, J. Org. Chem. **50**, 2972 (1985).

[9] C. A. Buser, C. W. Mallory, F. B. Mallory, P. A. Beckmann, K. G. Conn, and K. M. Gullifer (unpublished results).

[10] P. S. Allen and C. J. Howard, Mol. Phys. **16**, 311 (1969).

[11] J. Haupt and W. Müller-Warmuth, Z. Naturforsch. Teil A **24**, 1066 (1969).

[12] A. M. I. Ahmed and R. G. Eades, J. Chem. Soc. Faraday Trans. 2 **68**, 1337 (1972).

[13] A. M. I. Ahmed, R. G. Eades, T. J. Jones, and J. P. Llewellyn, J. Chem. Soc. Faraday Trans. 2 **68**, 1316 (1972).

[14] E. Rössler and H. Sillescu, Chem. Phys. Lett. **112**, 94 (1984).

[15] J. Haupt and W. Müller-Warmuth, Z. Naturforsch. Teil A **23**, 208 (1968).

[16] W. H. Flygare, *Molecular Structure and Dynamics* (Prentice–Hall, New Jersey, 1979).

[17] F. B. Mallory and C. W. Mallory, Org. React. **30**, 1 (1984).

[18] R. D. Haworth, J. Chem. Soc. 1125 (1932).

[19] C. K. Bradsher and R. W. H. Tess, J. Am. Chem. Soc. **61**, 2184 (1939).

[20] J. Cologne and A. Arsac, Bull. Soc. Chim. France **1956**, 445.

[21] J. E. Anderson and W. P. Slichter, J. Phys. Chem. **69**, 3099 (1965).

[22] P. A. Beckmann, Chem. Phys. **63**, 359 (1981).

[23] P. A. Beckmann, J. W. Emsley, G. R Luckhurst, and D. L. Turner, Mol. Phys. **50**, 699 (1983).

[24] F. Noack, NMR Basic Princ. and Prog. **3**, 81 (1971).

[25] R. G. Gordon, Adv. Magn. Reson. **3**, 1 (1968).

[26] A. M. Albano, P. A. Beckmann, M. E. Carrington, F. A. Fusco, A. E. O'Neill, and M. E. Scott, J. Phys. C **16**, L979 (1983).

[27] D. W. Davidson and R. H. Cole, J. Chem. Phys. **19**, 1484 (1951).

[28] S. Clough, Physica **136**, 145 (1986).

[29] M. Polak and D. C. Ailion, J. Chem. Phys. **67**, 3029 (1977).

[30] O. Edholm and C. Blomberg, Chem. Phys. **56**, 9 (1981).

[31] S. Clough and A. Heidemann, J. Phys. C **13**, 3585 (1980).

[32] J. Kowalewski and T. Liljefors, Chem. Phys. Lett. **64**, 170 (1979).

[33] O. Edholm and C. Blomberg, Chem. Phys. **42**, 449 (1979).

[34] C. Brot, Chem. Phys. Lett. **3**, 319 (1969).

[35] J. S. Waugh and E. I. Fedin, Sov. Phys. Solid State **4**, 1633 (1963).

[36] S. Clough, A. Heidemann, A. J. Horsewill, J. D. Lewis, and M. N. J. Paley, J. Phys. C **15**, 2495 (1982).

[37] S. Clough, P. J. McDonald and F. O. Zelaya, J. Phys. C **17**, 4413 (1984).

[38] E. C. Reynhardt, J. C. Pratt, and A. Watton, J. Phys. C **19**, 919 (1986).

[39] S. Emid, Chem. Phys. Lett. **72**, 189 (1980).

[40] S. Clough, Chem. Phys. Lett. **80**, 389 (1981).

[41] S. Emid, Chem. Phys. Lett. **80**, 393 (1981).